Published by
NIGERIAN SOCIETY OF PHYSICAL SCIENCES
Available online @ https://asr.nsps.org.ng/index.php/asr

African Scientific Reports 4 (2025) 332

African Scientific Reports

Investigation of direct normal irradiance and total cloud cover connection over Nigeria using satellite data

Louis Tersoo Abiem*, Tertsea Igbawua, Jacob Tersugh Adawa

Department of Physics, Joseph Sarwuan Tarka University Makurdi, Nigeria

Abstract

This study assessed the connection between direct normal irradiance (DNI) and total cloud cover (TCC) throughout Nigeria, a region with considerable yet underexploited solar energy potential. Daily DNI data from Modern-Era Retrospective Analysis for Research and Applications Version 2 (MERRA-2) and TCC data from the ERA5 reanalysis of the European Centre for Medium-Range Weather Forecasts (ECMWF) were aggregated into monthly means and analyzed across four climatological seasons. Seasonal variability was evaluated using standard deviation, while long-term trends were examined through simple linear regression, with statistical significance appraised at $p < 0.05$. Pearson's correlation coefficient was used to estimate DNI–TCC relationship. Results show that TCC peaked during JJA in the Af and Am climates, whereas DNI peaked in DJF and SON, particularly in the BSh and BWh regions. Variability in both DNI and TCC was highest in DJF and lowest in JJA. DNI variability was highest in the Aw zone and lowest in Am, while TCC variability peaked in the Aw and BWh zones and was lowest in Af and Am. Regression analysis revealed a strong inverse relationship between DNI and TCC in the Csb and BWh zones, while Af and Am exhibited complex interactions. Correlation analysis showed strongest negative relationship during DJF and JJA (mean $r = -0.73$), and weakest during MAM ($r = -0.33$). Trend analysis indicated a modest increase in DNI across all climate zones, with TCC decreasing except in Af. DNI values exceeding 400 W/m^2 were most likely in northern zones during DJF and SON but low in the south.

DOI:10.46481/asr.2025.4.3.332

Keywords: Direct normal irradiance, Total cloud cover, Seasonal variability, Long-term trend

Article History :
Received: 08 June 2025
Received in revised form: 03 December 2025
Accepted for publication: 03 December 2025
Published: 22 December 2025

1. Introduction

Nigeria has great potential for solar energy resources, as evidenced by its average annual global horizontal irradiation of between 1,600 and 2,200 kWh/m^2, with the northern region of the country having the highest values (over 2,000 kWh/m^2). The country's technological potential for solar photovoltaic (PV) is estimated by the International Renewable Energy Agency (IRENA) at 210 gigawatts (GW), taking into account that only 1% of the eligible land can be used for project construction [1]. Since the direct normal irradiance (DNI) is highest in northern Nigeria, this region has potential for concentrated solar power (CSP) of about 88.7 GW [2]. In spite of this, the nation is currently dealing with severe energy issues that range from uneven consumption patterns, an unstable and inefficient supply, to a lack of technological capability and inefficient use, while solar technology failed to meet

*Corresponding author Tel. No.: +234-703-068-7840.
Email address: abiem.lot@uam.edu.ng (Louis Tersoo Abiem)

the required input to the energy mix of 14% in 2008, 23% in 2015, and if the trend continues, 36% in 2030 as projected by the presidential committee on power development [3], largely because solar energy potential remains untapped [4].

By using concentrated solar power (CSP) technology and photovoltaic (PV) collectors, electricity can be generated from these resources [5, 6]. Only the direct beam portion of the solar resource can be used by CSP technology, with very few exceptions. For CSP plants to be powered, direct sunlight must be concentrated, which is why the beam radiation known as the Direct Normal Irradiance (DNI) is so important. Solar irradiation is reflected by clouds, aerosols, and other elements of the atmosphere, creating indirect or diffuse radiation. The variation of solar radiation is connected with attenuation in the atmosphere, mostly from clouds [7]. Because of clouds varying optical depth, they decrease the quantity of irradiance that reaches the earth surface. For example, photovoltaic array output of solar power generation can be reduced by up to 50–80% when there are impenetrable clouds over them. It has also been demonstrated that sporadic cloud cover over a CSP plant results in rapid changes in power output [8]. This results in transient voltage variations and wears down the distribution feeder's line equipment, leading to a rise in the cost of maintenance. These variations in solar energy management could necessitate the use of a backup power source, raising operating expenses. Forecasts of solar irradiation are therefore required for efficient grid management [9]. By anticipating and adjusting for power variations, short-term (< 5 h) irradiance prediction plays a crucial role in grid integration. Also, for the purpose of plant siting, evaluating the viability of a solar project, and taking seasonal variations in energy production and consumption into consideration, longer-term (> 10 years) irradiance projection is meaningful [10, 11]. For people planning to invest in or work in the solar energy industry, solar resource assessments are essential when considered collectively.

The most significant obstacle to solar irradiance predictions is understanding the intermittent nature of solar irradiation, which is closely linked with the movement of clouds [12]. But atmospheric circulations with intricate land and ocean dynamics control the movement of clouds. The heating and moistening of the atmosphere as well as surface heating are linked to the spread of clouds. Our knowledge of the climate and clouds in the future is constrained by the stochastic feedback caused by fluctuating atmospheric circumstances [13].

A recent study used coupled ocean–atmosphere climate models to investigate the effects of projected changes for the 21st century in temperature and irradiance on the power output of PV and CSP. They discovered that the changes in CSP output were greater than the changes in PV output in Nigeria from 2010 to 2080. The majority of the changes in CSP output was caused by changes in irradiance, while the majority of the changes in PV output was caused by changes in temperature [14]. Since there is increasing interest in the building of CSP plants in Nigeria [4, 15], this article evaluates how variations in cloud quantities affect direct normal irradiation (DNI) variability throughout Nigeria. Investigating how Nigeria's climate and weather affect cloud formation is crucial to understanding cloud variability.

While clouds fluctuate throughout the day primarily as a result of land and ocean convection, seasonal and decadal variations in cloud cover are linked to climate change. Olaniran *et al*. used meteorological datasets from the National Aeronautics and Space Administration to study the effects of cloudiness on surface radiation budget and temperature in Nigeria from 1983 to 2018. They observed that there were decreasing trends in net radiation (R) and increasing trends in cloud cover, with the least value obtained in the wet season. Variations in cloud cover accounted for 21 to 26% of changes in R and 14% of temperature fluctuations. The surface radiation budget was significantly perturbed by these variations [16].

Neher *et al*. studied on photovoltaic power potential in West Africa using long-term satellite data observed that the past 35 years have seen a considerable fluctuation in solar irradiation in West Africa, especially in the Sahel and Sahara regions. The highest solar irradiation was found in the Sahara and Sahel zone, where there was less temporal variability and a positive trend. Lower solar irradiance, with a negative trend and greater temporal variability, was experienced in southern West Africa. Because of this unpredictability, photovoltaic systems were impacted; PV outputs were higher in the Sahara and Sahel zones [17]. Also, in a study, solar radiation data obtained by remote sensing from 25 sites across Nigeria's five climatic zones were studied by Osinowo *et al*. Data from 16 locations were compared with 26-year mean monthly and daily data on solar radiation recorded on the ground. The satellite data and the ground-measured data were found to be in good agreement. Global irradiance frequency distribution was also studied. The findings indicated that between 15.01 and 20.01 MJ/m^2/day, irradiation was present in 46.88% and 40.6% of the days in the tropical rainforest and mangrove swamp forest, respectively. The coefficients of variations for irradiance were high throughout all climatic zones, but low mean values were observed in July and August. In Northern and Southern locations, contour maps showed high and low global sun irradiance and clearness index values, respectively [18].

Falayi and Rabiu established an empirical correlation for the computation of global solar radiation at eight distinct locations in Nigeria using monthly mean daily data on temperature, cloud cover, and global solar radiation at the locations. They compared the expected and observed results under different climate and geographic conditions and found that the primary determinant of the quantity of direct beam solar energy that reaches the earth's surface was clouds. Consequently, places with higher density of clouds got less solar radiation than those without clouds [19]. Danso *et al*. investigated the occurrence and variability of cloud cover types in WA using CERES passive satellite observations and ERA5 reanalysis. They studied the seasonal developments of high, middle, low, and total cloud cover and observed that both products agreed on the seasonal and spatial existence of cloud cover, but CERES presented lower values of cloud fraction than ERA5, partially due to the satellite sensor's inability to detect optically thin clouds. Southern WA was found to be cloudier than other parts of the region in all seasons, with mean TCC fractions of 70 and 80% for CERES and ERA5 respectively during the monsoon season [20].

Elliston *et al*. have recently reported on the occurrence and length of uncommon phenomena, such as prolonged periods of dense cloud cover that result in low solar insolation over parts of Australia caused by large-scale atmospheric circulation [21]. In a similar vein, Cheung *et al*. used factor analysis to examine solar irradiance data from several surface stations throughout Australia in order to identify trends in solar absorption by clouds. They discovered that different geographic areas connected to synoptic phenomena alter the cloud cover [22]. Troccoli and Morcrette also demonstrated how cloud cover and background climatic factors affect the accuracy of direct solar radiation predictions made by models over particular Australian locales [23].

Global seasonal climate is known to be influenced by several patterns of variability, primarily cloud cover and precipitation. While El Niño Southern Oscillation (ENSO), Indian Ocean Dipole (IOD), and Southern Annular Mode (SAM) primarily affect the Southern Hemisphere, the North Atlantic Oscillation (NAO) affects mainly the Northern Hemisphere [24, 25]. Abiem *et al*. used regression and correlation analysis on satellite remote sensing and gridded observation data to evaluate changes in Nigeria's climate. The temperature, precipitation, and top net solar radiation trends were shown to have negative, zero, and positive correlations respectively. El Niño Southern Oscillation (ENSO) and temperature had an indirect link with top net solar radiation but no direct relationship [26].

It's unclear if ENSO, temperature, and precipitation patterns alone can explain the significant variations in DNI over Nigeria over a variety of climate zones. To comprehend the changes in irradiance (especially DNI) linked to cloud variations across many temporal and geographical dimensions, more research is necessary. In order to address the gaps in the literature about the relationship between cloud intermittency and DNI variability—a crucial topic for CSP installations in Nigeria—this study makes use of satellite data. The study will clearly address the following concerns because it is essential to understand this link in order to improve Nigeria's energy plans and solar energy installations: What seasonal differences exist in cloud cover and DNI in Nigeria? How much does the variation in DNI relate to the variation in cloud cover over Nigeria? What is the pattern of cloud amounts and DNI in Nigeria from 2001 to 2022? What underlying factors lead to these seasonal variations?

2. Materials and methods

2.1. Study area

Nigeria, a country in West Africa stands out for its diverse climate and geographical makeup. The country is located between latitude 4°N and 14°N of the equator and between longitude 3°E and 15°E of the Greenwich meridian, and it has a total area of 923,768 km^2. The country shares boundary with Benin republic on the west and Cameroon on the east, while Chad and Niger share a northern border and with the Gulf of Guinea in the south. The southern part of Nigeria experiences consistent humidity, large cloud cover and low solar irradiation whereas the northern part of the country experiences drier weather with distinct wet and dry seasons. Locations around the nation experience wildly varying amounts of rainfall. The Sahel in the north requires irrigation because of a more severe dry season, characterized by high solar irradiation and aerosols, while the Niger Delta region in the south benefits from lush vegetation due to its heavy cloud cover and rainfall. The terrain consists of plains, plateaus, and mountains, with the Jos Plateau in the center and the Adamawa Plateau in the northeast standing out. Coastal plains and mangrove swamps in the southwest contribute to the nation's abundant biodiversity. Climate patterns are influenced and the seasonal monsoons are supported by the interactions between the Atlantic Ocean, the Gulf of Guinea, and the southern coast of Nigeria. These interactions impact the country's ecology, agriculture, and way of life. The country is divided into thirty-six (36) states and Abuja (the Federal Capital Territory) [27].

The study area is shown in Figure 1 with partitions displaying Koppen climate classifications: Af, Am, Aw, BSh, BWh, and Csb, which stand for Tropical Rainforest, Tropical Monsoon, Tropical Savanna, Hot Semi-Arid Climate (Steppe), Hot Desert, and Mild Temperature with Dry/Warm Summer Climates. High temperatures and year-round, heavy rainfall are hallmarks of the tropical rainforest climate. A Tropical Monsoon Climate with distinct wet and dry seasons is represented by the Am classification. Aw denotes a Tropical Savanna climate with dramatic contrasts between arid and rainy summers. In the direction of arid areas, BSh denotes a Hot Semi-Arid Climate (Steppe), which is characterized by high temperatures, significant day-night temperature fluctuations, and a discernible dry season. Extreme daytime temperatures, little precipitation, and no real rainy season are characteristics of the BWh, or hot desert climate. On the other hand, Csb describes Warm Temperate Mediterranean Climates, which are situated on the western borders of continents and have pleasant summers with a noticeable difference in precipitation between the two seasons.

2.2. Sources of data

To investigate the relationship between direct normal irradiation (DNI) and total cloud cover (TCC) over Nigeria, two main data sources were used; (i) daily all sky surface shortwave downward direct normal irradiance was acquired from the archives of the Modern-Era Retrospective Analysis for Research and Applications, Version 2 (MERRA-2) obtained from https://power.larc.nasa.gov/data-access-viewer/; (ii) total cloud cover was downloaded from the archives of the European Centre for Medium range Weather Forecast Reanalysis – version 5 (ERA-5) obtained from https://www.ecmwf.int/en/forecasts/dataset/ecmwf-reanalysis-v5.

Also, nino 3.4 dataset was extracted from sea surface temperature anomalies calculated using the Extended Reconstructed Sea Surface Temperature version 5 (ERSST.v5) and obtained from https://www.ncei.noaa.gov/access/monitoring/enso/sst. The summary

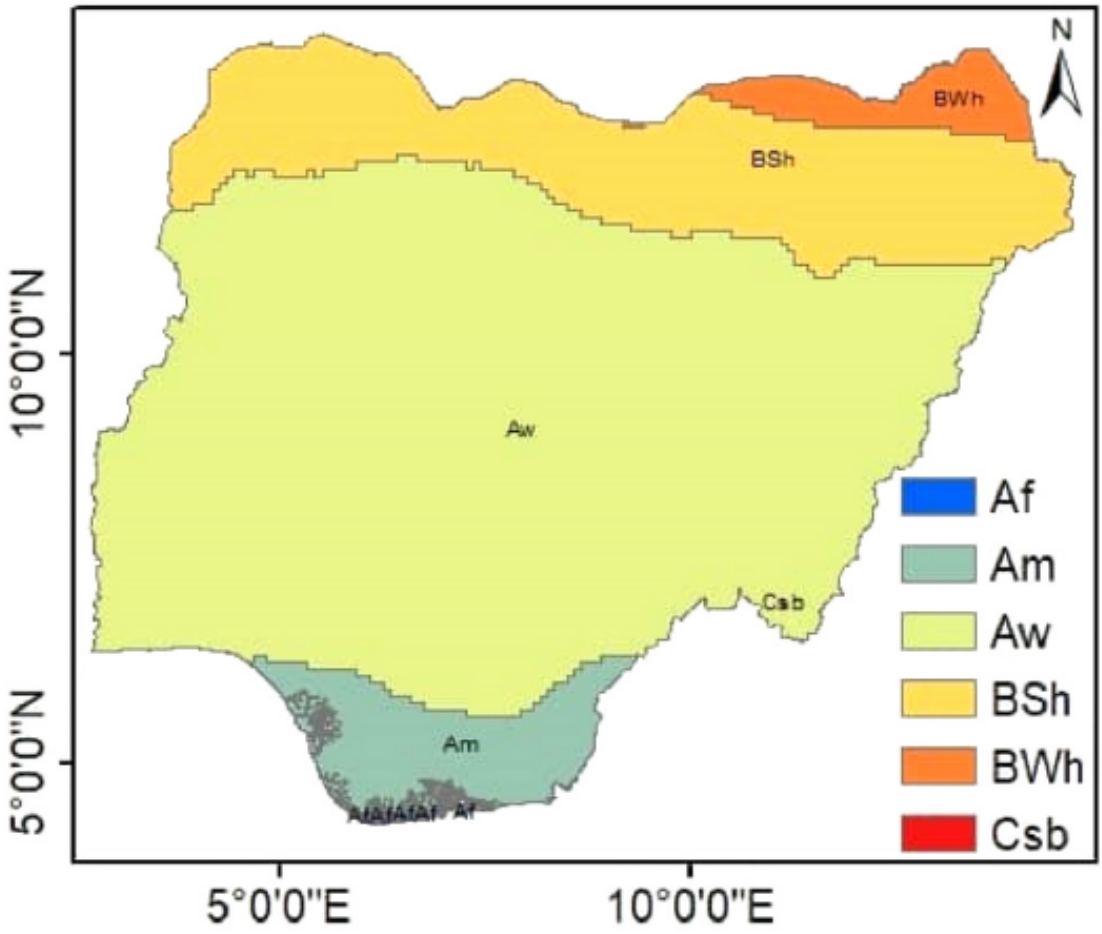

Figure 1: The study area with partitions displaying Koppen climate classifications Af, Am, Aw, BSh, BWh, and Csb [27].

Table 1: Data sets.

S/N	Data	Source	Resolution	Resampled	Time period
1	DNI	MERRA-2	$0.5° \times 0.625°$	$0.038° \times 0.038°$	2001–2022
2	TCC	ERA-5	$0.25° \times 0.25°$	$0.038° \times 0.038°$	2001–2022
3	Nino 3.4	ERSST.v5	$0.25° \times 0.25°$	$0.038° \times 0.038°$	2001–2022
4	Koppen Climate Data	[28]	$0.01° \times 0.01°$	Shapefile	

of the data sets is provided in Table 1. Furthermore, Beck *et al.* provided a qualitative framework for characterizing the climates of particular regions within the study area by integrating the Koppen climate classification [28]. This can be accessed at https://www.gloh2o.org/koppen/.

2.3. Data analysis

2.3.1. Seasonal variations of TCC and DNI

To understand the seasonal variations in TCC and DNI climatology, the daily datasets were first grouped into monthly and divided into four seasons: dry [December–January–February (DJF)], end of dry/beginning of wet [March–April–May (MAM)], wet [June–July–August (JJA)] and end of wet/beginning of dry [September–October–November (SON)]. Variability was ascertained using standard deviation (equation (1)) from the seasonal mean for both DNI and TCC. This is in line with a number of earlier researches that employed standard deviation to study variability [29–32].

$$\sigma = \sqrt{\frac{1}{N}\sum_{i=1}^{N}\left(\mathrm{DNI}_i - \overline{\mathrm{DNI}}\right)^2}, \tag{1}$$

where σ is the standard deviation, N is the number of data points, DNI_i is each individual value in the dataset, and $\overline{\mathrm{DNI}}$ is the population mean. DNI in equation (1) was subsequently replaced with TCC values and mean for the computation of standard deviation in TCC.

2.3.2. Trend analysis

In order to calculate the long-term trends, seasonal anomalies were computed to eliminate seasonality from the data. By finding the difference between the average for a particular season and the average for all years of that season, the deseasonalized seasonal anomaly was calculated. Loeb *et al.*; Prasad and Davies respectively had used a similar procedure to compute deseasonalized monthly anomalies of satellite measured irradiances and effective cloud heights [31, 33]. Trend was calculated through the use of simple linear regression (equation (2)) of the deseasonalized datasets, with $p < 0.05$ values taken to be statistically significant. In this study, TCC was the independent and DNI the dependent variable. Likewise, DNI and TCC as the dependent and time (year) as the independent variable for the computation of long term DNI and TCC trends. Journée, *et al.* used this method to compute trends in surface solar radiation over the Benelux [30].

$$\mathrm{DNI} = \varepsilon + \mathrm{TCC} \cdot \beta, \tag{2}$$

where DNI is the dependent variable, TCC is the independent variable, ε is the intercept, and β is the slope.

The slope, β, was determined using equation (3).

$$\beta = \frac{\sum \left(\mathrm{TCC}_i - \overline{\mathrm{TCC}}\right)\left(\mathrm{DNI}_i - \overline{\mathrm{DNI}}\right)}{\sum \left(\mathrm{TCC}_i - \overline{\mathrm{TCC}}\right)^2}. \tag{3}$$

2.3.3. Correlation of TCC with DNI

Pearson's correlation coefficient, which measures the magnitude and direction of the linear relationship between two variables over a certain time period, was used to evaluate DNI – TCC connections. The DNI and TCC data were re-gridded using linear interpolation to match the dataset resolutions. $p < 0.05$ is considered statistically significant unless otherwise indicated.

$$r = \frac{\sum_{i=1}^{n} \left(\mathrm{TCC}_i - \overline{\mathrm{TCC}}\right)\left(\mathrm{DNI}_i - \overline{\mathrm{DNI}}\right)}{\sqrt{\sum_{i=1}^{n} \left(\mathrm{TCC}_i - \overline{\mathrm{TCC}}\right)^2} \cdot \sqrt{\sum_{i=1}^{n} \left(\mathrm{DNI}_i - \overline{\mathrm{DNI}}\right)^2}}, \tag{4}$$

where n is number of observations.

2.3.4. Correlation of nino 3.4 with TCC

This study also correlates the Niño 3.4 region, defined as the central equatorial Pacific area between 5°N and 5°S latitude and 120°W and 170°W longitude, with TCC (using equation (4)) to examine their relationship in Nigeria. The index is an essential metric used to assess the El Niño–Southern Oscillation (ENSO) phenomenon, which significantly impacts worldwide climate patterns. Sea surface temperature anomalies (SSTa) in this region were employed to detect the occurrence of El Niño (warm phase) and La Niña (cold phase) phenomena, and SSTa values surpassing 0.49 were designated as El Niño periods, reflecting warmer-than-normal instances for five consecutive months, whilst values below -0.49 were classified as La Niña periods, denoting cooler-than-normal instances for the same timeframe. SSTa levels between -0.5 and 0.5 were taken as normal.

3. Results and discussion

3.1. Monthly average DNI over Nigeria

The monthly average DNI across Nigeria's Koppen climates, showing trends and variations, essential for understanding the nation's solar energy potential throughout the year is in Figure 2.

Figure 2 shows that the arid climates, especially BWh and BSh, consistently exhibited the highest DNI throughout the year, with BWh peaking at 498.82 W/m^2 and 484.02 W/m^2 in November and December respectively, while BSh reached 514.21 W/m^2 and 502.36 W/m^2 during the same months. Even during their lowest levels in July and August, DNI remained considerably high—307.82 W/m^2 and 306.84 W/m^2 respectively for BWh, and 313.41 W/m^2 and 300.73 W/m^2 for BSh—indicating remarkable solar potential throughout the year. The Mediterranean Csb zone showed significant monthly fluctuations, with a high of 503.85 W/m^2 in December and a notable drop to 169.49 W/m^2 in August, which closely aligns with cloud cover. The tropical regions generally presented lower DNI values, likely due to persistent cloudiness and other environmental factors. The Af ranged from a low value of 133.21 W/m^2 in July to a high value of 281.14 W/m^2 in December, whereas Am varied from 142.18 W/m^2 in July to 307.86 W/m^2 in December. The Aw (savanna) climate illustrated a middle ground, with peak values of 448.74 W/m^2 in December and a decrease to 185.09 W/m^2 in August. Across all zones, December recorded the highest DNI values, followed by November and January, while lowest DNI values were observed in August, followed by July and June. The arid zones provided higher irradiance throughout the year, and have strong potential for solar energy use. This aligns with previous works by Ogunmodimu and Marquard; Ogunjo *et al.* [2, 34]. Osinowo *et al.* also noted elevated global sun irradiance in northern regions and diminished levels in southern areas [18].

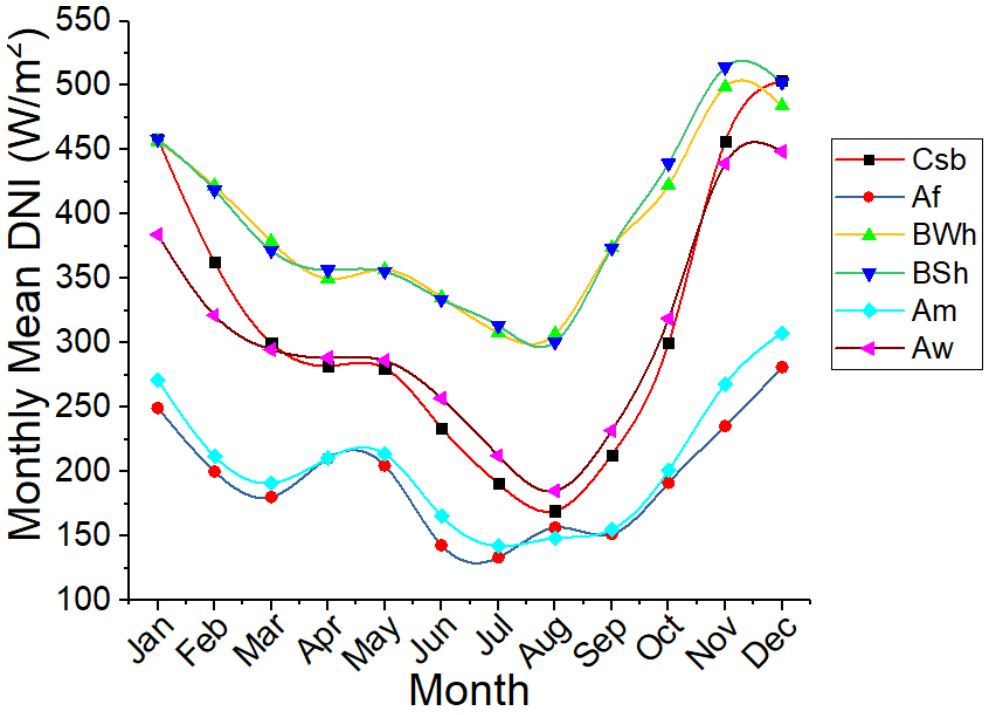

Figure 2: Monthly average DNI over Nigeria's Koppen climate zones. The data extend from 2001–2022.

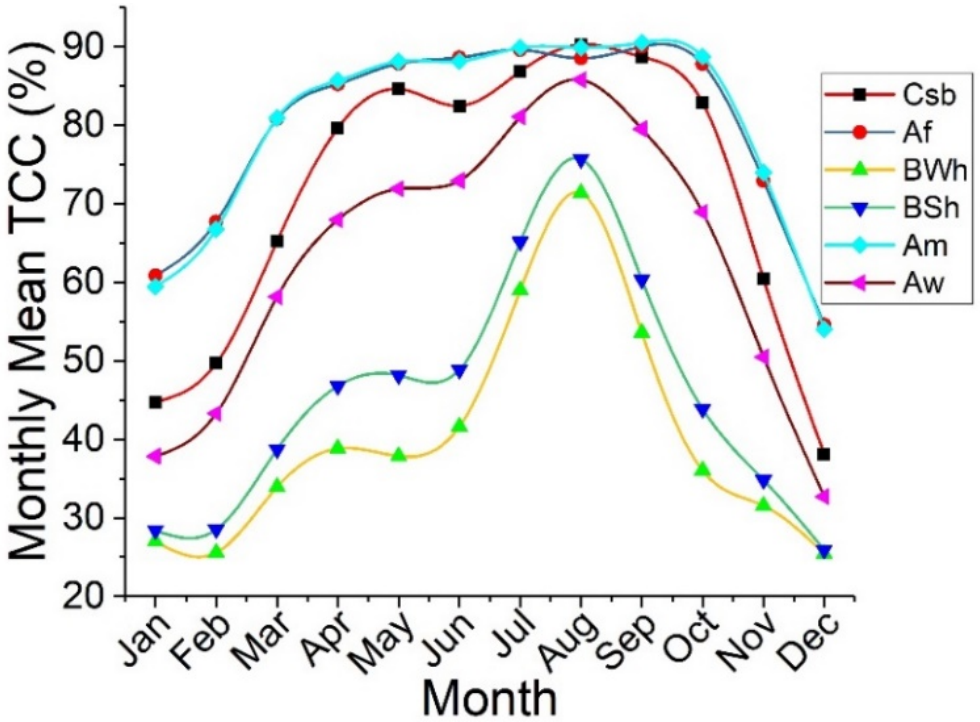

Figure 3: Monthly average TCC over Nigeria's Koppen climate zones. The data extend from 2001–2022.

3.2. Monthly average TCC over Nigeria

The monthly average TCC across Nigeria's Koppen climatic classification, illustrating trends and variations by region, essential for understanding the nation's cloud cover throughout the year are presented in Figure 3.

Figure 3 showed that the tropical climates, especially Af and Am, demonstrated consistently high cloud cover year-round, reaching their highest levels during the end of the wet season. Af peaked at 88.91% in July and 90.02% in September, while Am hits 89.31% in August and 90.50% in September, signifying persistent atmospheric moisture and equatorial convection. Aw also regis-

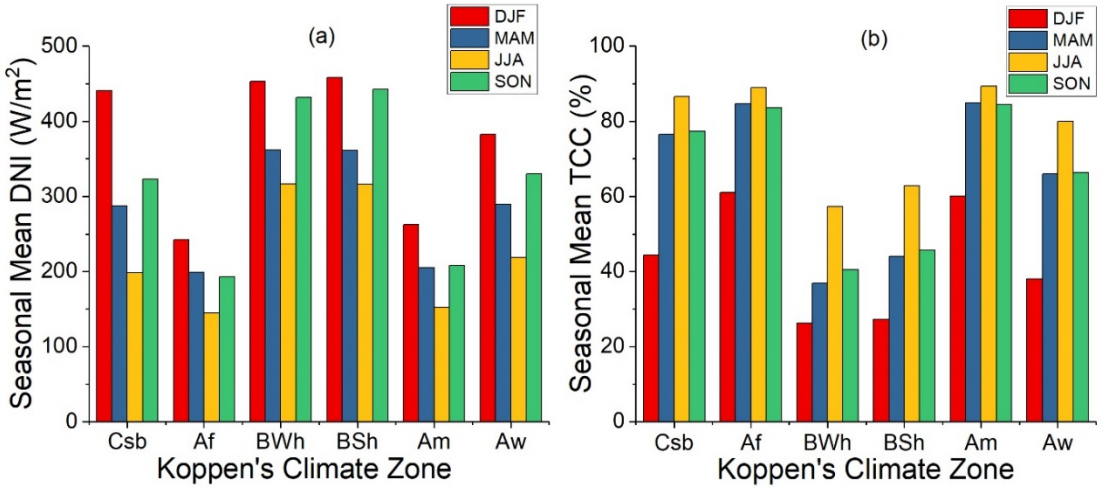

Figure 4: Seasonal mean (a) DNI and (b) TCC across Nigeria's six Köppen climate zones. The data extend from 2001–2022.

tered significant TCC, rising from 38.03% in January to 85.79% in August, revealing a pronounced wet season. Conversely, the desert climates, BWh and BSh consistently possessed the lowest TCC, especially during DJF, with BWh falling to 25.44% in December, and BSh at 25.92% in the same month. These areas witnessed a seasonal uptick, reaching peaks of 71.37% and 75.69% respectively in August, —still exhibiting much clearer skies compared to the tropical climates. The Mediterranean (Csb) climate displayed a significant seasonal variation. TCC escalated sharply from a minimum of 38.14% in December to a maximum of 90.30% in August, reflecting a corresponding seasonal decrease in solar irradiance. Across all zones, December recorded the lowest TCC values, followed by January and February, while highest TCC values were observed in August, except for Af and Am zones who recorded the highest TCC values in September. In summary, Figure 3 reveal an inverse correlation between TCC and DNI, where reduced cloud cover in the arid and Mediterranean regions align with higher and more consistent solar energy potential, whereas tropical regions, with high cloudiness throughout the year, suffered diminished DNI. Ohunakin *et al.* observed that the highest cloud cover in Nigeria from 1981 to 2010 occurred in July, August, and September, with average rates of 65%, 80%, and 95% in the northern, central, and southern regions, respectively, coinciding with the peak rainy season [35]. Additionally, Falayi and Rabiu noted that coastal areas exhibited greater cloud density and less irradiance compared to the northern regions of the country [19].

3.3. Seasonal mean DNI and TCC over Nigeria

The seasonal mean DNI and TCC values across Nigeria's Koppen climate zones, illustrating trends and variations by region, essential for understanding the nation's solar energy potential and cloud cover throughout the year are presented in Figure 4.

Figure 4 (a) depicts the seasonal changes in DNI across Nigeria's six Köppen climate zones. Arid areas such as BWh and BSh showed consistently high DNI throughout the year, peaking in DJF at 452.65 W/m^2 and 457.85 W/m^2, respectively, and maintaining elevated levels in SON (431.75 W/m^2 and 442.49 W/m^2) and JJA (316.63 W/m^2 and 315.97 W/m^2), respectively. The Mediterranean Csb zone demonstrated a comparable seasonal trend, with a peak DNI of 440.51 W/m^2 in DJF and a significant decrease to 198.02 W/m^2 in JJA, likely due to increased cloud cover. In contrast, the tropical regions displayed lower and more fluctuating DNI due to persistent cloudiness and seasonal precipitation. The Af zone varied between 144.24 W/m^2 in JJA and 242.30 W/m^2 in DJF, while Am varied from 152.01 W/m^2 to 262.22 W/m^2 over the same seasons. The Aw climate zone had moderate DNI values, reaching a maximum of 382.65 W/m^2 in DJF and dropping to 218.13 W/m^2 in JJA. These trends indicate that drier climates benefit from greater and more consistent solar radiation, emphasizing their significant potential for solar energy use throughout the year.

Figure 4 (b) illustrates the seasonal differences in TCC across Nigeria's six Köppen climate zones. The tropical climates consistently displayed high TCC, especially during JJA, with Af reaching 88.91%, Am at 89.31%, and Aw at 79.97%. Even during DJF, these areas retained considerable cloud cover—Af and Am stayed high (61.05 and 60.10% respectively), while Aw declined to 38.03%, its lowest seasonal mark. In contrast, dry climates (BWh and BSh) showed the least TCC, particularly in DJF (26.19% and 27.22%, respectively), which aligns with their elevated DNI during the same season. TCC in these arid regions increased during JJA to 57.34% for BWh and 62.83% for BSh. The Mediterranean Csb climate demonstrated distinct seasonal variation, with TCC at its lowest in DJF (44.31%) and peaking in JJA at 86.54%, closely following the pattern of its DNI. These findings support an inverse correlation between TCC and DNI: areas and seasons characterized by lower cloud cover tend to receive greater amounts of direct solar radiation.

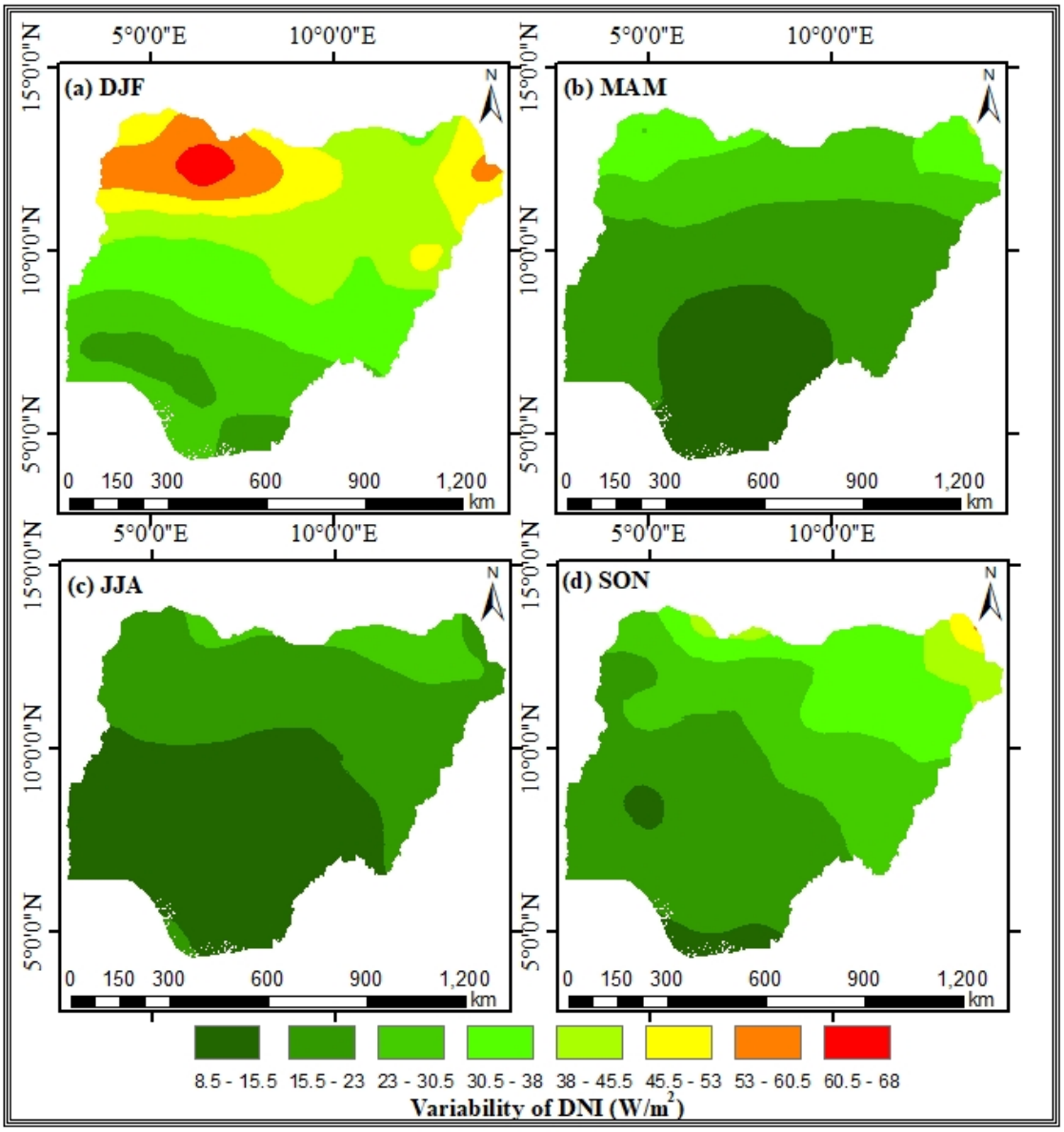

Figure 5: Variability (standard deviation) of DNI over Nigeria for each season: (a) Dry (DJF), (b) End of dry (MAM), (c) Wet (JJA) and (d) End of wet (SON). The data extends from 2001–2022.

3.4. Seasonal variability of DNI over Nigeria

The spatial distribution of DNI variation over Nigeria for the seasons is presented in Figure 5. The Figure shows that the highest variation in DNI was observed during the DJF season, particularly in the BSh and BWh zones in the northwest and northeast, with measurements exceeding 60 W/m^2; the Aw zone exhibited the widest range (20–66 W/m^2), followed by the BSh zone (40–64 W/m^2), while the southern zones (Af and Am) displayed less variability (~23 W/m^2) due to more stable cloud and rainfall patterns. In MAM, variability decreased across the country, with the BWh and BSh zones recording approximately 40 W/m^2 and 35 W/m^2, respectively; the Aw zone saw a decrease to a maximum of 32 W/m^2, while the Af and Am zones reported the lowest values (13 and 14 W/m^2, respectively), indicating more consistent irradiation. During JJA, the rainy season, DNI variability was at its lowest—Aw reduced to a maximum of 22 W/m^2, while the Af and Am zones were at around 15 and 13 W/m^2, respectively, and the BWh zone noted the highest variability at just 26 W/m^2. Variability increased again in SON, with notable variations in BWh (30–55 W/m^2), BSh (~45 W/m^2), and Aw (~40 W/m^2), while the Af and Am zones remained stable at around 14 and 16 W/m^2, respectively. These seasonal patterns are consistent with the findings of Osinowo *et al.* [18], who observed significant irradiance variability but low average values in July and August. Ogunmodimu and Marquard [2], also reported highest DNI variability in northern Nigeria with a potential for 88.7 GW CSP. The findings emphasize the importance of considering seasonal variations and regional discrepancies when planning the location of solar energy infrastructure in Nigeria, particularly for CSP systems.

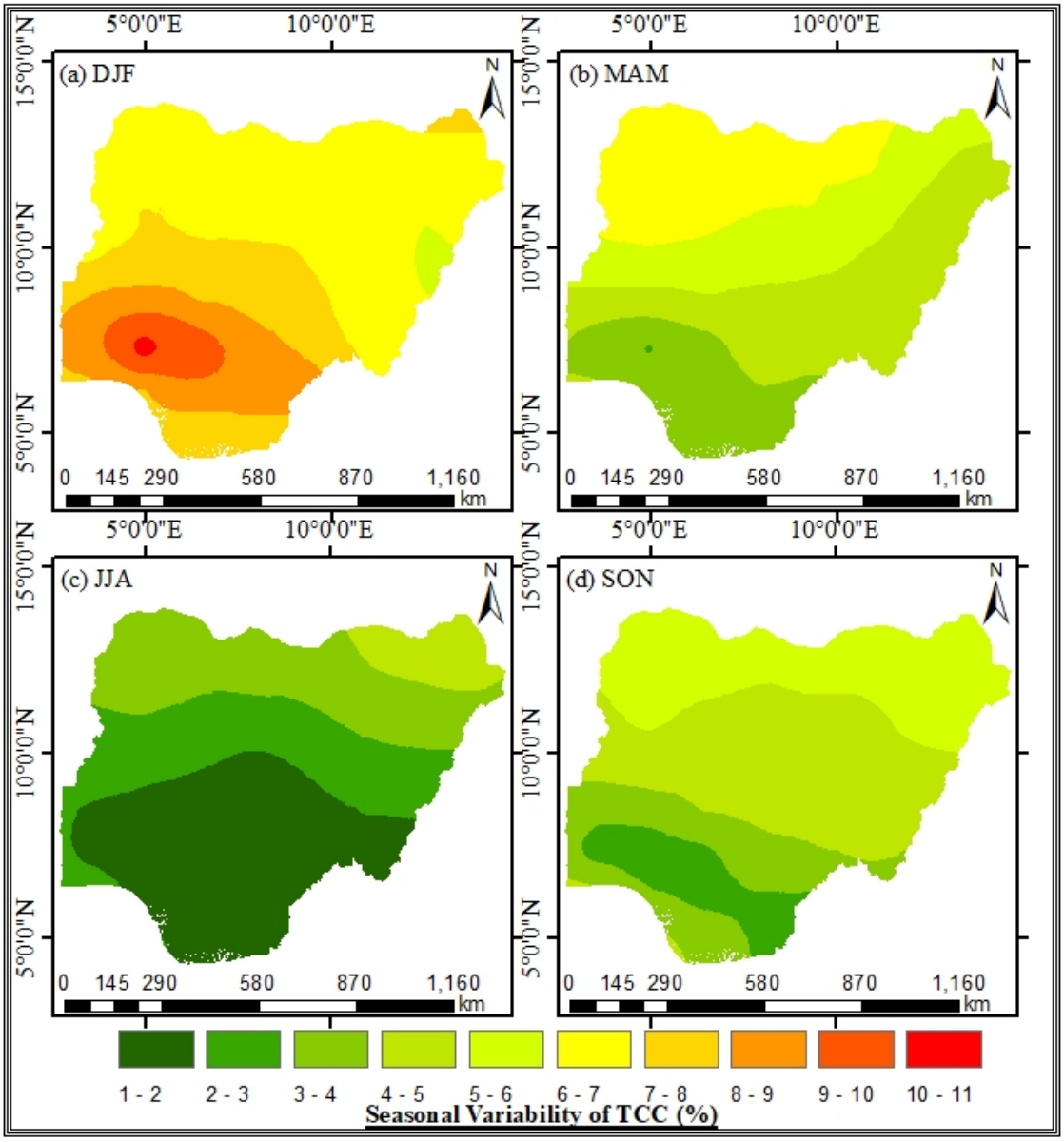

Figure 6: Variability (standard deviation) of TCC over Nigeria for each season: (a) Dry (DJF), (b) End of dry (MAM), (c) Wet (JJA) and (d) End of wet (SON). The data extends from 2001–2022.

3.5. Seasonal variability of TCC over Nigeria

The spatial distribution of TCC variation over Nigeria for each season is presented in Figure 6.

It shows that in the DJF season, the Aw zone exhibited the greatest TCC variations (8 – 11%), whereas the BSh and BWh zones displayed the lowest variability (~6%), attributable to the arid, dusty Harmattan winds. The Af and Am zones exhibited modest variations (7 – 8%) associated with consistent coastal moisture. In MAM, there was a nationwide decrease in TCC variability; the Af and Am zones experienced reductions to 3–4%, whereas the Aw, BWh, and BSh areas displayed moderate variability (4–7%) likely due to early convective activities. The Csb zone maintained a stable TCC variability of around 4.5%, potentially attributed to orographic influences.

In JJA, during the peak of the rainy season, variability was at its lowest (1–2%) in the Af, Am, and Csb zones because of constant cloud cover, while the BWh and BSh zones recorded slight variability of up to 4.5%, and Aw fluctuated between 1–4%. During SON, TCC variability experienced a slight uptick across Aw, BSh, and BWh zones (reaching 5.5%) as moisture levels decreased; meanwhile, Af and Am zones also showed a modest rise (2–4%), with Csb remaining at around 4%. Generally, TCC variability was most pronounced in the DJF season and least in the JJA season, with the Aw zone exhibiting the most significant seasonal variations. These trends are consistent with regional climate behavior and support findings by Danso *et al.* [20] which noted increased cloudiness in southern West Africa during the monsoon. Ohunakin *et al.* [35] also observed that maximum (low variability) cloud cover in

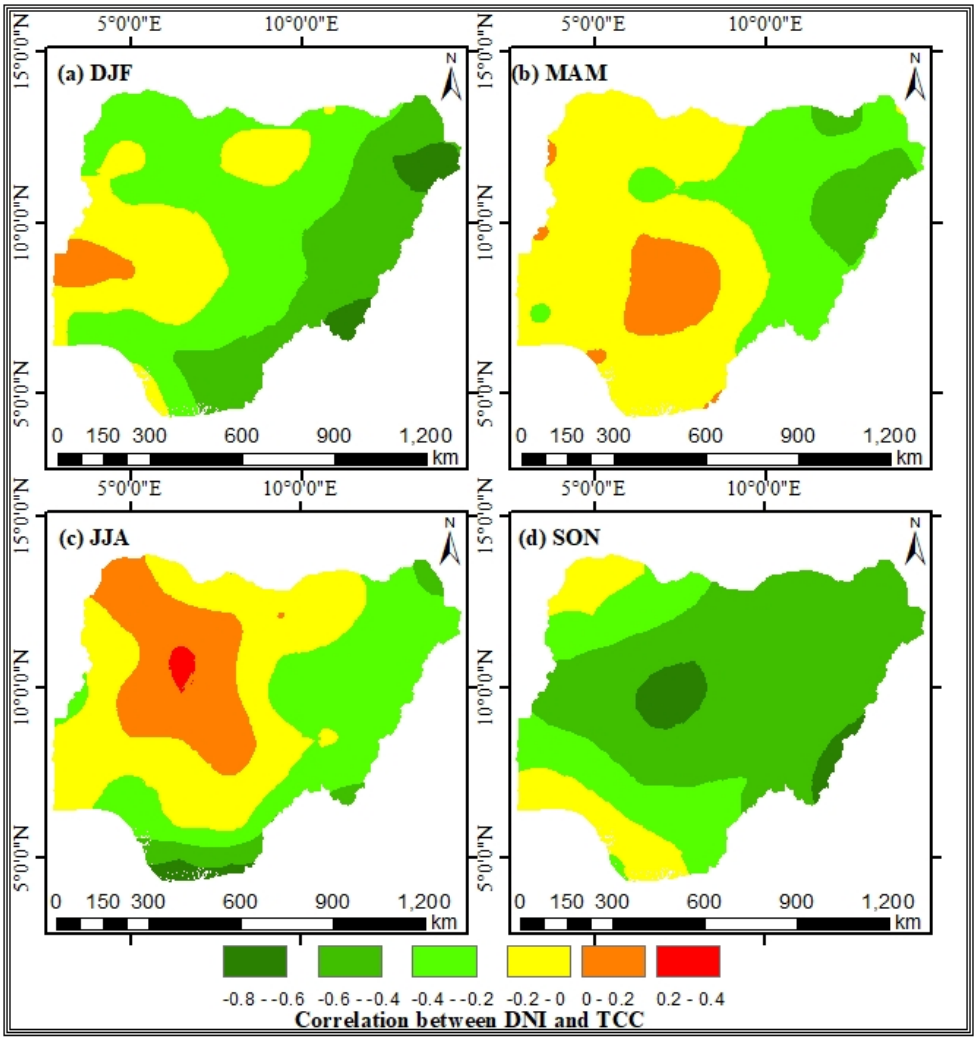

Figure 7: Correlation between DNI and TCC over Nigeria for each season: (a) Dry (DJF), (b) End of dry (MAM), (c) Wet (JJA) and (d) End of wet (SON). The data extend from 2001–2022.

Nigeria from 1981 to 2010 occurred in July, August, and September, with mean rates of 65%, 80%, and 95% in the northern, central, and southern regions, respectively.

3.6. Correlation between DNI and TCC over Nigeria

The spatial distribution of the correlation between DNI and TCC over Nigeria for each season is presented in Figure 7.

Figure 7 shows that in the DJF season, all climate zones exhibited predominantly negative correlations, particularly in the Csb, parts of BSh, and Aw zones (correlation < -0.75), indicating that increased cloud cover significantly diminished DNI levels. The Aw zone also had areas of positive correlation, implying localized conditions where clouds did not entirely block solar radiation. The BWh and Am zones displayed moderately negative correlations, while the Af zone recorded weaker negative values, suggesting the influence of other environmental factors. In the MAM season, the Af and Am showed weak negative values, whereas Aw, BWh, and BSh exhibited correlations ranging from -0.46 to 0.18, with sporadic weak positive values that pointed to scattered clouds not significantly impacting DNI. During the JJA, the most substantial negative correlation (-0.7) was found in Af and Am zones due to thick cloud cover, while weaker correlations in BSh, BWh, and Aw indicated clearer skies and higher DNI; Csb experienced moderate negative correlations associated with drying conditions. The SON season recorded negative correlations lessened in most areas as cloud cover gradually decreased; Af and Am presented weak correlations (-0.2 to -0.4), while Aw, BSh, and BWh showed moderate negative values due to fluctuating cloudiness.

Throughout all seasons, the most pronounced negative correlations (-0.5 to -0.8) between DNI and TCC were observed in southern coastal regions during JJA and in the northeast during DJF and SON. Weaker correlations (> -0.3) in northern and central areas indicate additional atmospheric factors at play. Positive correlations were noted in central Nigeria during DJF, MAM, and JJA, suggesting localized influences, while SON exhibited none. Correlations were generally more robust in the eastern regions

and exhibited greater variability in the west, aligning with Olaniran *et al.* [16]; Falayi and Rabiu who also noted that locations in the coastal region exhibited greater cloud density and received less solar radiation compared to those in the northern section of the country [19].

3.7. DNI and TCC trend over Nigeria

The minimum, maximum, mean and annual average of DNI and TCC seasonal trends over Nigeria for each season is presented in Table 2.

Table 2: DNI and TCC trend over Nigeria for each season: DJF, MAM, JJA and SON. The data extend from 2001–2022.

Seasonal DNI Trend (W/m^2/month)													
		DJF			MAM			JJA			SON		Av
Köppen	Min	Max	Mean	Min	Max	Mean	Min	Max	Mean	Min	Max	Mean	
Csb	0.537	0.552	0.545	0.4396	0.497	0.469	0.217	0.236	0.227	1.210	1.235	1.222	0.616
Af	0.644	0.934	0.795	0.891	0.931	0.907	0.802	0.907	0.878	-0.240	-0.110	-0.198	0.595
BWh	0.142	3.905	2.038	-0.176	1.613	0.765	-2.183	1.885	-0.690	1.881	7.039	3.573	1.422
BSh	0.179	3.879	1.646	-0.285	1.350	0.386	-2.202	0.985	-1.310	0.734	4.752	2.163	0.721
Am	0.109	1.076	0.664	0.5799	0.999	0.914	0.363	0.906	0.766	-0.210	0.906	0.329	0.668
Aw	-0.539	3.245	0.560	-0.692	1.015	0.113	-1.836	0.983	-0.300	-0.020	2.839	0.905	0.320
Seasonal TCC Trend (%/month)													
		DJF			MAM			JJA			SON		Av
Köppen	Min	Max	Mean	Min	Max	Mean	Min	Max	Mean	Min	Max	Mean	
Csb	-0.228	-0.226	-0.227	-0.145	-0.139	-0.142	-1.361	-1.328	-1.344	-0.080	-0.078	-0.079	-0.448
Af	-0.121	-0.078	-0.090	-0.325	-0.291	-0.299	-0.956	-0.176	-0.577	0.676	0.837	0.751	-0.054
BWh	-0.424	-0.387	-0.412	0.131	0.331	0.256	-0.262	-0.169	-0.201	-0.386	-0.023	-0.238	-0.149
BSh	-0.454	-0.316	-0.393	0.015	0.332	0.138	-0.838	-0.101	-0.310	-0.390	0.337	-0.030	-0.149
Am	-0.210	-0.072	-0.152	-0.584	-0.276	-0.363	-2.550	0.390	-0.531	0.203	0.914	0.680	-0.091
Aw	-0.458	-0.168	-0.278	-0.745	0.249	-0.117	-2.771	0.233	-1.079	-0.328	0.717	0.161	-0.328

Table 2 shows that seasonal trends of DNI and TCC throughout Nigeria, categorized by Köppen's climatic zones, exhibited clear spatial and temporal differences. In the DJF season, the BWh and BSh zones demonstrated the highest trends in DNI, with average values of 2.038 W/m^2/month and 1.646 W/m^2/month respectively, reflecting clear skies typical of the Harmattan season. In contrast, the Aw zone showed a negative minimum value (−0.539 W/m^2/month), indicating the effects of dust and low solar angles. During the MAM season, moderate declines in DNI trends were observed in the BWh (maximum of 1.613 W/m^2/month) and BSh (maximum of 1.35 W/m^2/month) zones. Except for the Af and Am zones, average values decreased as cloud cover increased with the beginning of rainfall. The JJA season experienced a notable drop in DNI trends across all zones, particularly in BWh and BSh, which recorded significant negative minima (−2.183 and −2.202 W/m^2/month, respectively), due to substantial cloud coverage. On the other hand, the Af and Am zones had comparatively higher average DNI values (0.878 and 0.766), although they were still reduced. The SON season indicated an increase in DNI, especially in BWh (average: 3.573) and BSh (2.163), attributable to diminishing cloud cover and drier weather. Generally, BWh recorded the highest annual average DNI (1.422), followed by BSh (0.721) and Csb (0.616), while Aw had the lowest average (0.320), illustrating obvious seasonal variations. Dogara *et al.* also observed increasing DNI trends in Zaria, northern Nigeria [36].

TCC trends generally reflected the opposite of DNI. In the DJF season, all zones experienced a reduction in cloud cover, with Aw (−0.458 %/month) and BSh (−0.454 %/month) exhibiting the most significant negative changes, promoting higher DNI. MAM recorded increasing cloud cover trends in BWh (0.256 %/month) and BSh (0.138 %/month), corresponding with convective development, while Af and Am zones showed continued decreases in TCC. JJA presented sharp negative trends in TCC for Aw (−2.771 %/month) and Am (−2.550 %/month), signifying clearer skies toward the end of the raining season. During the SON season, TCC trends were mixed, with Af (mean of 0.751%/month) and Am (mean value of 0.680) displaying increases, suggesting maintained moisture, while northern zones like Aw and BSh showed variable trends. Annually, the most significant declines in cloud cover were observed in the Csb and Aw zones (−0.448 and −0.328 %/month, respectively), whereas Af remained nearly constant (−0.054). These trends agree with Sato *et al.* who found that topography greatly influences cloud formation, with developments frequently happening over unstable terrains due to heightened elevation and proximity to the water, leading to diminished solar irradiation [37]. Edokpa *et al.* reported higher mean cloud cover in the south than northern Nigeria [38].

3.8. Mean DNI vs time series over Nigeria

The time series of mean DNI in Nigeria (Figure 8) demonstrates the temporal trends and long-term variability crucial for evaluating the stability and reliability of solar energy supplies nationwide.

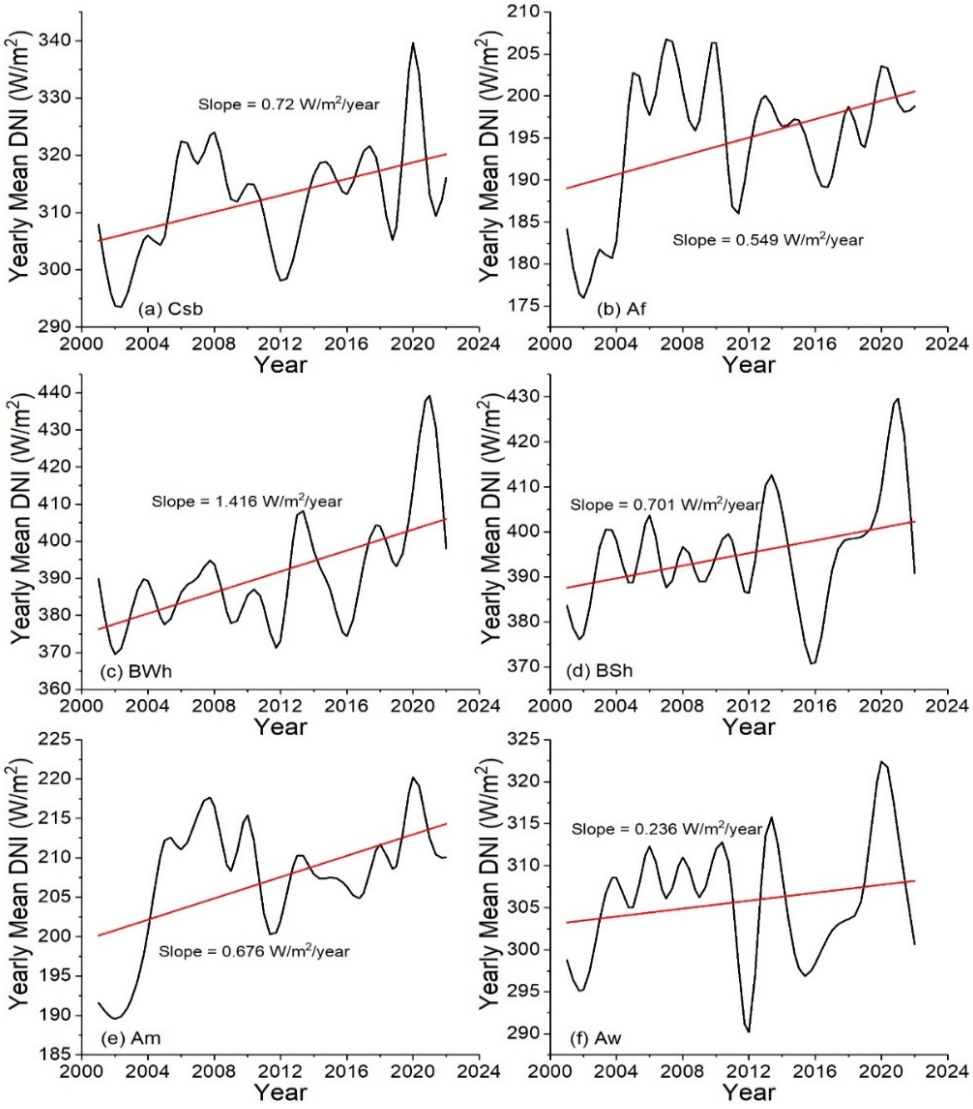

Figure 8: Mean DNI vs time series plots over Nigeria's Köppen climate zones. The data extend from 2001–2022.

The annual average DNI from 2001 to 2022 exhibits a steady upward trajectory across six Köppen climate zones as illustrated in time series graphs (Figure 8). The most substantial increase was recorded in the BWh zone, with a slope of +1.416 W/m^2/year, and DNI increased from 389.91 W/m^2 in 2001 to 439.35 W/m^2 in 2021, before dropping to 398.07 W/m^2 in 2022. The Csb zone followed with a slope of +0.72 W/m^2/year, beginning at 307.88 W/m^2 in 2001, reaching a peak of 339.63 W/m^2 in 2020, and ending at 316.09 W/m^2 in 2022. The BSh zone experienced an increase from 383.68 W/m^2 in 2001 to a peak of 429.65 W/m^2 in 2021, ultimately finishing at 390.84 W/m^2 in 2022, with a slope of +0.701 W/m^2/year. In the tropical monsoon (Am) zone, there is a more gradual rise (slope +0.676 W/m^2/year), with values climbing from 191.60 W/m^2 in 2001 to 220.25 W/m^2 in 2020, then slightly decreasing to 210.10 W/m^2 in 2022. The Af zone, known for extensive cloud cover, saw DNI grow from 184.21 W/m^2 in 2001 to a maximum of 206.36 W/m^2 in 2010, stabilizing at 198.80 W/m^2 by 2022, yielding a slope of +0.549 W/m^2/year. And the Aw zone experienced a more modest increase (slope +0.236 W/m^2/year), rising from 298.78 W/m^2 in 2001 to 322.41 W/m^2 in 2020, and ending at 300.66 W/m^2 in 2022. These consistent rise in DNI across all climate zones depicts a broader climatic trend toward clearer skies, which could enhance surface warming and improve the feasibility of solar energy—especially in arid and semi-arid regions. This rise in DNI aligns with diminishing TCC, indicating that lower cloudiness permits more solar radiation to the earth's surface.

3.9. Mean TCC vs time series over Nigeria

The time series of mean TCC over Nigeria (Figure 9) demonstrates temporal variations and long-term trends that affect solar radiation availability and facilitate climate-related evaluations.

From 2001 to 2022, TCC across Nigeria displayed unique spatial and temporal trends with majority of decreasing trend, apart from the Af zone. The Af and Am zones showed the highest TCC values, generally between 75% and 82%, indicating persistent

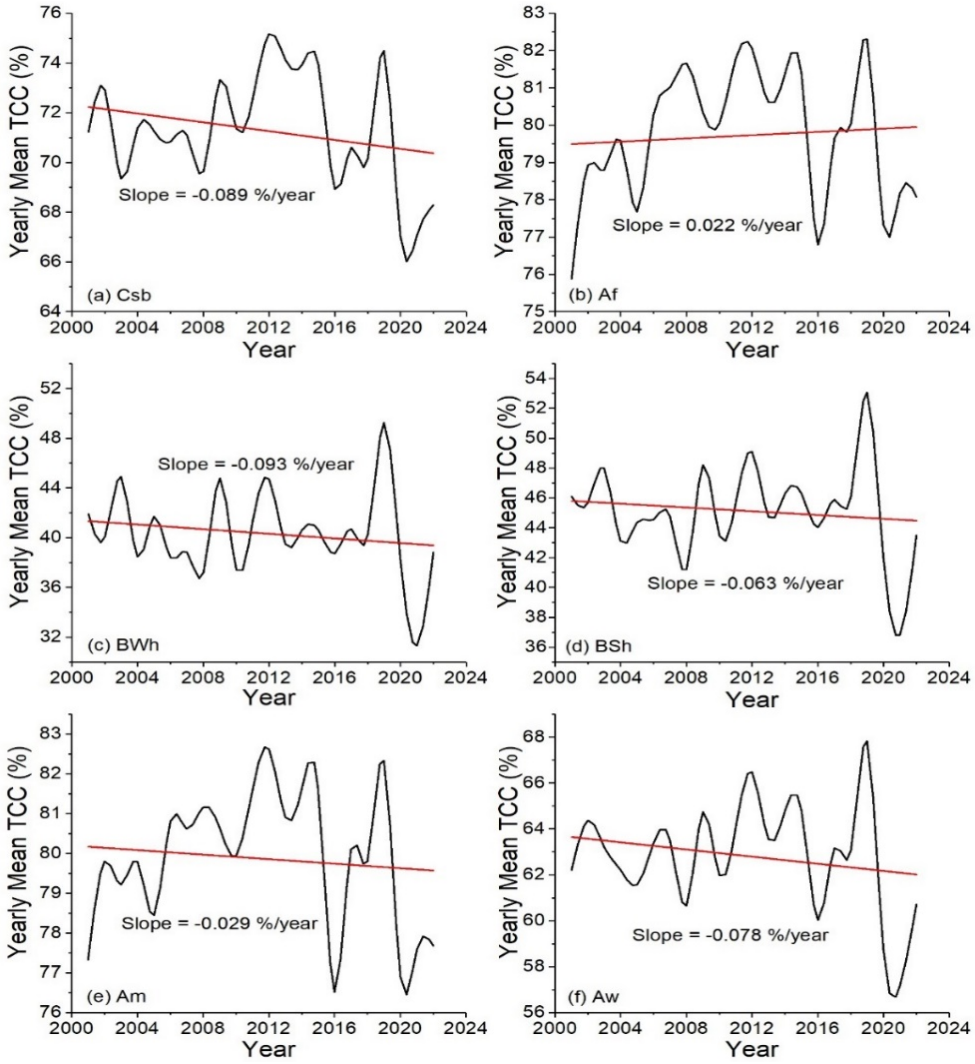

Figure 9: Mean TCC vs time series plots over Nigeria's Köppen climate zones. The data extend from 2001–2022.

cloudiness due to considerable atmospheric moisture. In contrast, the drier BWh and BSh zones recorded the lowest TCC values, from 31.3% to 49.2%, signifying frequent clear skies and dry conditions. The Csb and Aw zones presented intermediate TCC levels, ranging from 68.3% to 75.2% and 57.2% to 67.8%, respectively. Significant interannual fluctuations were observed, with particularly low TCC recorded in 2016 and 2021, especially in BWh, where TCC fell to 31.3%. On the contrary, 2019 was characterized by increased cloudiness across many zones, with TCC reaching 82.31% in Af, 82.33% in Am, and higher-than-normal values in BWh (49.24%) and BSh (53.07%), likely influenced by moisture inflow associated with ENSO. Analyzing the trends shows a decline in TCC across most climate zones, with the most significant reductions occurring in BWh (−0.093%/year), Csb (−0.089%/year), and Aw (−0.078%/year), indicating a rise in clear-sky conditions that could enhance solar energy use. The BSh zone experienced a moderate decrease of −0.063%/year, while the Am zone demonstrated mild decline of −0.029%/year. Only the Af zone showed a slight increase in TCC (+0.022%/year), suggesting that cloudiness remains relatively stable in Nigeria's humid areas. These temporal trends point to a general decline in cloud formation processes across Nigeria, particularly in the drier northern regions and transitional areas, likely affected by regional aridification and large-scale climate influences such as ENSO.

3.10. Regression slope between DNI and TCC over Nigeria

The regression slope between DNI and TCC in Nigeria (Figure 10) illustrates the influence of cloud cover variations on solar radiation across various climatic zones.

The analysis of regression slopes between DNI and TCC throughout Nigeria reflects the responses of solar irradiance to variations in cloudiness. The Af zone recorded only positive regression slopes ranging from 0.25 W/m^2 to 0.73 W/m^2, suggesting that the frequent presence of clouds in this region had minimal effect on DNI. This indicates localized conditions in which clouds did not completely obstruct sun radiation, or the impact of other environmental factors. The Aw zone, which predominates central Nigeria,

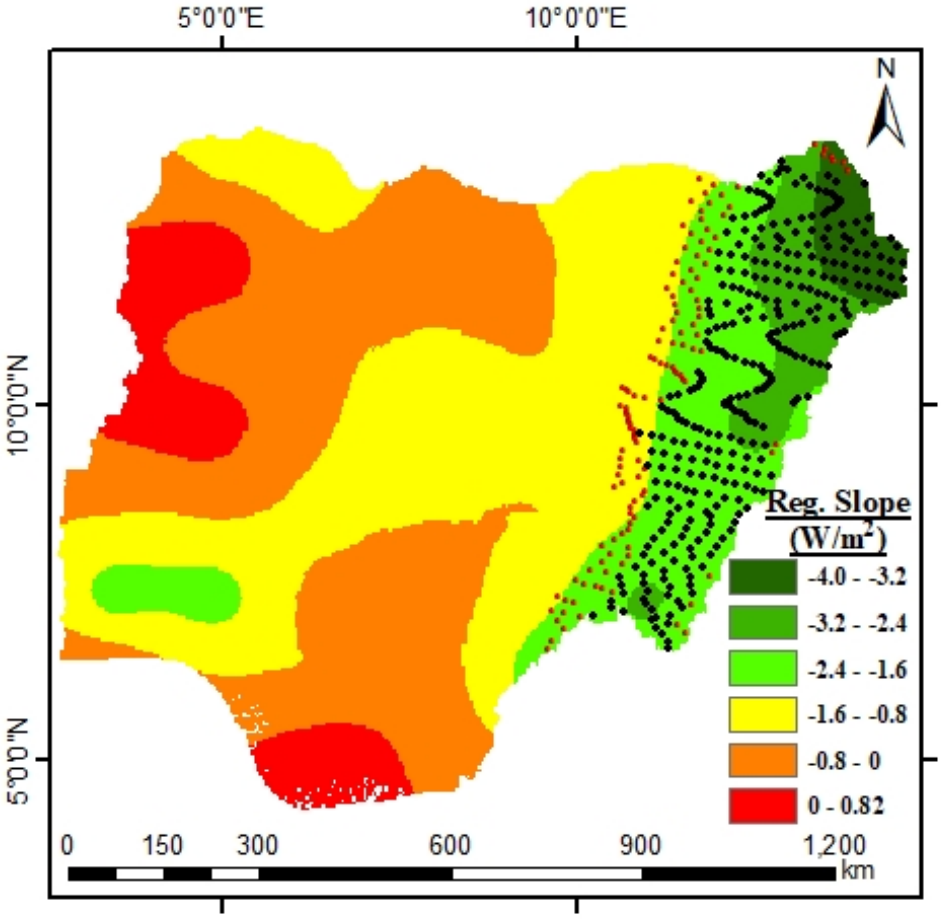

Figure 10: Spatial distribution of DNI versus TCC regression slopes over Nigeria.

revealed a range of moderately negative slopes (-2.86 W/m^2) to a weak positive slope (0.57 W/m^2), and a mean of (-0.99 W/m^2). In this zone, DNI exhibited a more pronounced response to cloud fluctuations, consistent with the region's distinct wet and dry seasons. In contrast, the BSh region showed distinctly negative slopes (minimum of -3.87 W/m^2, and mean of -1.36 W/m^2), indicating that even minor increases in cloud cover significantly diminished solar radiation in this region. This trend was more evident in the BWh zone with all negative slopes ranging from -3.97 to -0.7 W/m^2, and a mean slope of -2.38, signifying that typical clear skies made the impact of cloud ingress on DNI even more substantial. Notably, the Csb zone also displayed a stable and significantly negative mean slope (-2.36). On the contrary, the Am had a weakly negative mean slope (-0.16 W/m^2), and a minimum of -1.89 W/m^2, but recorded the highest positive value of 0.82 W/m^2, implying a more intricate interaction—likely influenced by high humidity, diffuse radiation, and varying cloud types. On a general note, the regression analysis demonstrates a clear inverse correlation between DNI and TCC in the arid and Mediterranean regions, whereas tropical areas such as Af and Am showed less pronounced or more complex relationships. Stippling shows significant differences ($p < 0.05$). The statistically significant regression slopes seen in northeastern Nigeria are presumably affected by the presence of highland terrains, including the Mambilla and Adamawa highlands. Medugu *et al*. observed that orographic lifting in elevated regions promotes organized cloud formation, resulting in more steady and predictable fluctuations in cloud cover. The combination of better air conditions and sharper irradiance contrasts enhances the negative correlation between DNI and TCC, leading to higher signal-to-noise ratios and statistically significant p-values [39].

3.11. Application of DNI to CSP

The growth of CSP largely relies on factors such as terrain, load, transmission structure, and fluctuations in DNI [40]. Nonetheless, the duration and strength of DNI are critical for the essential operation of CSP. Nigeria experiences around 6.5 hours of sunlight daily and lies within the high sunshine region [41]. According to the International Energy Agency, any form of CSP operation generally necessitates a minimum DNI of 1900 kWh/m^2/year [42]. For effective CSP functions in Nigeria, Ogunmodimu and Okoroigwe proposed a minimum DNI threshold of roughly 400 W/m^2 [4]. Figure 11 illustrates the likelihood of DNI intensity at 400 W/m^2 or higher during the daytime [indicated as P(DNI > 400 W/m^2)] through various seasons across Nigeria.

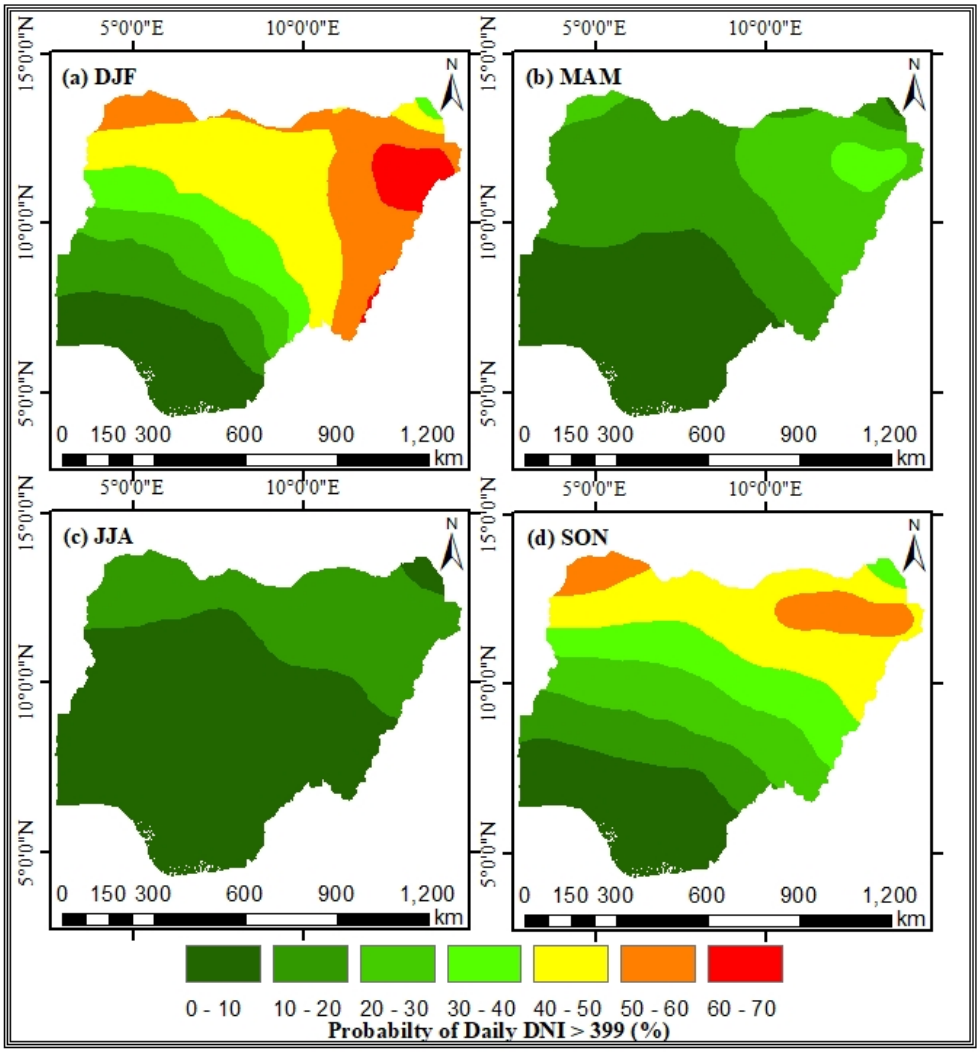

Figure 11: The probability of daily DNI ≥ 400 W/m^2 over Nigeria for each season: (a) Dry (DJF), (b) End of dry (MAM), (c) Wet (JJA) and (d) End of wet (SON). The data extend from 2001–2022.

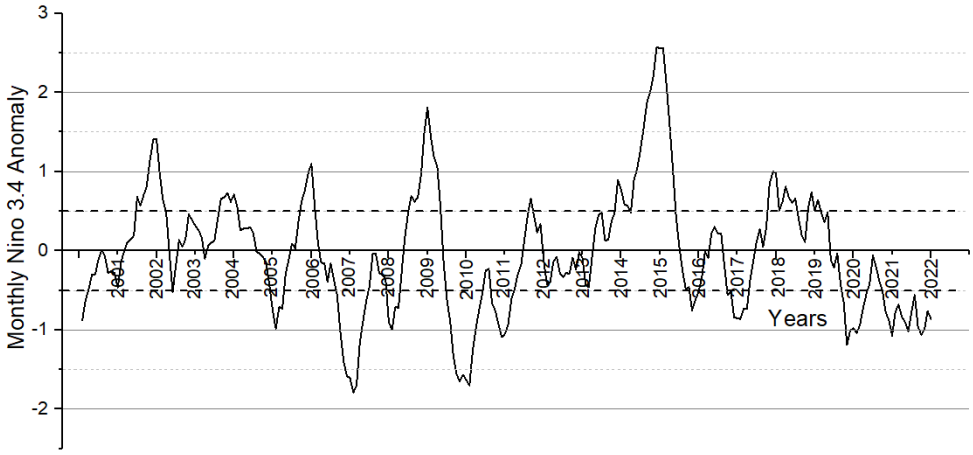

Figure 12: Time series of monthly El Niño 3.4 anomalies from 2001 to 2022.

The seasonal probability of daily DNI surpassing 400 W/m^2 reveals considerable spatial diversity, with the northern climate zones exhibiting greater potential for CSP. In the DJF season, the BWh and BSh zones displayed the highest probabilities—reaching

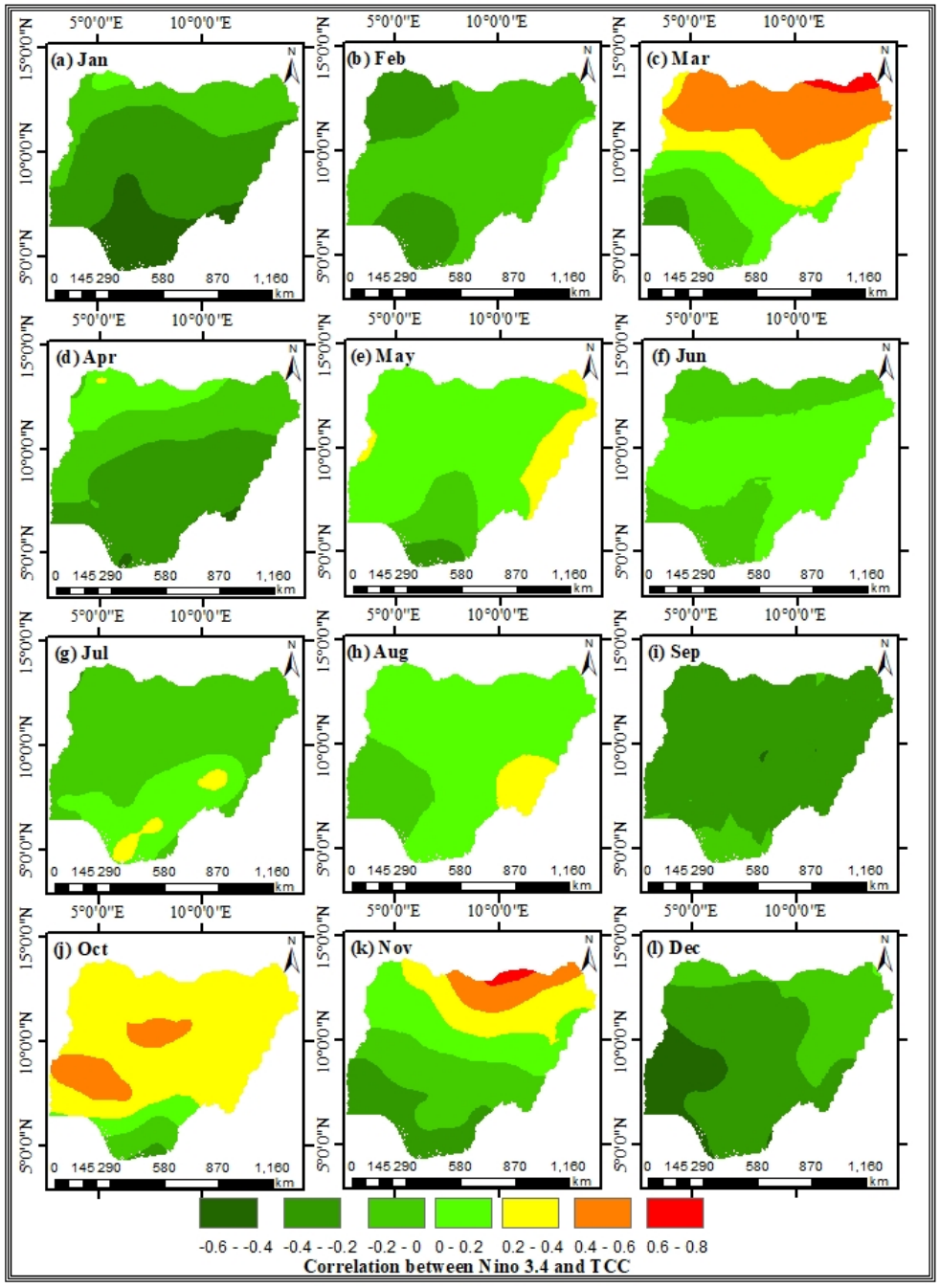

Figure 13: Monthly correlation between Nino 3.4 and TCC over Nigeria. The data extend from 2001–2022.

up to 55% and 64%, respectively—this could be due to clear skies and low cloud interference. Likewise, the northern Aw region achieved probabilities of up to 63%, while the southwestern part reported significantly lower chances (below 10%). On the contrary, the southern Af and Am regions had minimal probabilities (below 10%) due to persistent cloudiness and humidity. During the MAM season, the probabilities of DNI exceedance became more evenly distributed, ranging from 1–30% across the country. The northern and central regions (BWh, BSh, and Aw) continued to exhibit favorable CSP conditions, while coastal zones (Af and Am) remained under 5%. The JJA season, marked by heavy cloud cover and rainfall, witnessed the lowest exceedance probabilities, with most southern areas recording below 1% and northern zones like BWh, BSh, and Aw showing moderate values ($\leq$ 20%). The SON season experienced a resurgence in DNI probabilities as clouds diminished, with the BWh and BSh regions reporting between 40–60%, and the northern section of the Aw zone reaching up to 50%. The southwestern Aw, as well as areas in Af and Am, sustained probabilities below 10% due to relatively high humidity and cloud cover. Generally, these trends indicate that the northern regions of Nigeria—particularly during DJF and SON—are exceptionally suited for CSP development. These observations are consistent with findings

by Sambo [3], Ogunmodimu & Marquard [2], and Ogunmodimu & Okoroigwe [4], who noted that the DNI potential in northern Nigeria exceeds 88.7 GW.

3.12. Correlation of nino 3.4 with TCC

Figure 12 shows the time series of monthly Niño 3.4 SSTa from the year 2001 to 2022. It revealed notable El Niño events that occurred in 2002–2003, 2009–2010, and most notably in 2015–2016, during which the anomaly exceeded +2.5°C, constituting one of the most intense El Niño occurrences documented. Modest El Niño events also transpired from 2004-2005 and 2018-2019, exhibiting prolonged durations of positive anomalies marginally exceeding the threshold. In contrast, La Niña events occurred throughout various intervals, including 2007–2008, 2010–2011, 2011–2012, and most recently from 2020 to 2022.

The last episode indicates a sustained La Niña event characterized by persistent negative anomalies, with some approaching −1.5°C, implying significant cooling in the central Pacific. These cold episodes are linked to disturbances, including diminished rainfall in specific areas and heightened storm activity in others [43]. Neutral events, characterized by anomalies oscillating between −0.5°C and +0.5°C, are particularly observable during 2003–2004, 2013–2014, and segments of 2017. These intervals are distinguished by a relative lack of pronounced ENSO signals, signifying more stable oceanic conditions.

Figure 13 illustrates that the relationship between Niño 3.4 and TCC in Nigeria differed by region and month. In the dry DJF season, the southern and central areas experienced moderate negative correlations, with minimum values of −0.47 in Aw (December), −0.55 in Af (January), and −0.27 in Am (February), while the BWh region displayed negligible correlation. During March, strong positive correlations emerged in the northern region, peaking at 0.64, indicating increased cloud cover due to early moisture influx. These positive trends diminished in April, leading to a blend of moderately negative (−0.43) to weakly positive (0.22) correlations throughout the nation. Positive correlations appeared in BWh, BSh, and southeastern regions in May, whereas the southwestern areas showed weak negative values. The influence of ENSO was minimal in June, with primarily neutral to weakly negative correlations observed. In July, weak negative correlations re-emerged in the north, while Af exhibited weak positive values. August was marked by weak positive correlations across most areas, except for Am and southwestern Aw, which exhibited very weak negative trends. In September, weak to moderately negative correlations returned, particularly in Aw, while October presented a mix of weak negative and positive correlations, including moderate positives in central Aw. November recorded the strongest positive ENSO signal, with BWh reaching as high as 0.67, while Af and Am noted weak negative values around −0.37.

Generally, southwestern Aw consistently demonstrated strong negative correlations across multiple months, while BWh repeatedly showed strong positive correlations during transitional months, revealing a clear seasonal and spatial response of ENSO to TCC in Nigeria.

4. Conclusion

This study reveals that cloud cover has a substantial effect on solar irradiance throughout Nigeria, consistently resulting in a negative effect on Direct Normal Irradiance (DNI) in all seasons, with the most pronounced impacts seen during the dry (DJF) and wet (JJA) periods. Different climatic zones react patchily, with the Aw and BWh zones exhibiting the greatest variability in DNI. While there is generally an inverse relationship between Total Cloud Cover (TCC) and DNI, some occasional weak positive correlations indicate that factors such as cloud type and atmospheric conditions may play a role. Long-term trend analysis shows a slow rise in DNI during all the seasons, with the northern region experiencing the highest trend. The probability of DNI surpassing 400 W/m^2 is also greatest in the northern regions during dry periods, stressing the regions viability for solar energy projects. Additionally, ENSO events have a marked effect on TCC, which subsequently influences DNI, particularly in the Aw and BWh zones. In summary, the study provides valuable insights into how location, seasons, and climatic elements impact solar energy potential in Nigeria, offering important direction for energy policy, infrastructure development, and strategies for climate adaptation. Future studies should concentrate on explaining the effects of cloud types, aerosols, high-resolution DNI variability, and other climatic drivers to enhance modeling accuracy and optimize Nigeria's solar energy strategy within an ever-changing climate.

Data availability

Data will be made available upon reasonable request from the corresponding author.

Acknowledgment

The authors acknowledge NASA POWER (MERRA-2), ECMWF (ERA-5), NOAA (ERSST.v5), and Beck *et al.* (Köppen climate classification) for providing the datasets used in this study.

References

[1] IRENA-AfDB report: Energy Transition Central to Africa's Economic Future, 14 January 2022 Press Releases. https://primeprogressng.com/perspective/energy-transition-central-to-africas-economic-future-irena-afdb-report/.

[2] O. Ogunmodimu & A. Marquard, "CSP technology and its potential contribution to electricity supply in Northern Nigeria", International Journal of Renewable Energy Research **3** (2013) 529. https://dergipark.org.tr/tr/download/article-file/148304.

[3] A. S. Sambo, "Matching electricity supply with demand in Nigeria", International Association for Energy Economics **2008** (2008) 32. https://www.iaee.org/documents/newsletterarticles/408sambo.pdf.

[4] O. Ogunmodimu & E. C. Okoroigwe, "Solar thermal electricity in Nigeria: Prospects and challenges", Energy Policy **128** (2019) 440. https://doi.org/10.1016/j.enpol.2019.01.013.

[5] N. Boerema, G. Morrison, R. Taylor & G. Rosengarten, "High temperature solar thermal central-receiver billboard design", Solar Energy **97** (2013) 356. https://doi.org/10.1016/j.solener.2013.09.008.

[6] R. A. Taylor, P. E. Phelan, T. P. Otanicar, C. A. Walker, M. Nguyen & S. Trimble, "Applicability of nanofluids in high flux solar collectors", Journal of Renewable and Sustainable Energy **3** (2011) 023104-1. https://doi.org/10.1063/1.3571565.

[7] D. Yang, P. Jirutitijaroen & W. M. Walsh, "Hourly solar irradiance time series forecasting using cloud cover index", Solar Energy **86** (2012) 3531. https://doi.org/10.1016/j.solener.2012.07.029.

[8] K. M. Powell & T. F. Edgar, "Modeling and control of a solar thermal power plant with thermal energy storage", Chemical Engineering Science **71** (2012) 138. https://doi.org/10.1016/j.ces.2011.12.009.

[9] K. Stefferud, J. Kleissl & J. Schoene, "Solar forecasting and variability analyses using sky camera cloud detection & motion vectors", in *2012 IEEE Power and Energy Society General Meeting*, San Diego, CA, USA, 2012, pp. 1–6. https://doi.org/10.1109/PESGM.2012.6345434.

[10] S. Lohmann, C. Schillings, B. Mayer & R. Meyer, "Long-term variability of solar direct and global radiation derived from ISCCP data and comparison with reanalysis data", Solar Energy **80** (2006) 1390. https://doi.org/10.1016/j.solener.2006.03.004.

[11] F. R. Martins, E. B. Pereira, S. A. B. Silva, S. L. Abreu & S. Colle, "Solar energy scenarios in Brazil, part one: resource assessment", Energy Policy **36** (2008) 2853. https://doi.org/10.1016/j.enpol.2008.02.014.

[12] S. R. West, D. Rowe, S. Sayeef & A. Berry, "Short-term irradiance forecasting using skycams: motivation and development", Solar Energy **110** (2014) 188. https://doi.org/10.1016/j.solener.2014.08.038.

[13] A. A. Prasad, "Tropical thin cirrus from MISR: detection, validation and trends", Ph.D. dissertation, Department of Physics, University of Auckland, New Zealand, 2012. https://hdl.handle.net/2292/20579.

[14] J. A. Crook, L. A. Jones, P. M. Forster & R. Crook, "Climate change impacts on future photovoltaic and concentrated solar power energy output", Energy & Environmental Science **4** (2011) 3101. https://doi.org/10.1039/c1ee01495a.

[15] D. Akinyele, O. Babatunde, C. Monyei, L. Olatomiwa, A. Okediji, D. Ighravwe, O. Abiodun, M. Onasanya & K. Temikotan, "Possibility of solar thermal power generation technologies in Nigeria: Challenges and policy directions", Renewable Energy Focus **29** (2019) 24. https://doi.org/10.1016/j.ref.2019.02.002.

[16] J. M. Olaniran, A. A. Muritala, O. O. Emmanuel & A. S. Lukman, "Impacts of cloudiness on near surface radiation and temperature in Nigeria, West Africa", SN Applied Sciences **2** (2020) 2127. https://doi.org/10.1007/s42452-020-03961-y.

[17] I. Neher, S. Crewell, S. Meilinger, U. Pfeifroth & J. Trentmann, "Photovoltaic power potential in West Africa using long-term satellite data", Atmospheric Chemistry and Physics **20** (2020) 12871. https://doi.org/10.5194/acp-20-12871-2020.

[18] A. A. Osinowo, E. C. Okogbue, S. B. Ogungbenro & O. Fashanu, "Analysis of global solar irradiance over climatic zones in Nigeria for solar energy applications", Journal of Solar Energy **2015** (2015) 819307. https://doi.org/10.1155/2015/819307.

[19] E. O. Falayi & A. B. Rabiu, "Estimation of global solar radiation using cloud cover and surface temperature in some selected cities in Nigeria", Archives of Physics Research **2** (2011) 99. http://scholarsresearchlibrary.com/archive.html.

[20] D. K. Danso, S. Anquetin, A. Diedhiou, C. Lavaysse, A. Kobea & N. D. E Touré, "Spatio-temporal variability of cloud cover types in West Africa with satellite-based and reanalysis data", Quarterly Journal of the Royal Meteorological Society **145** (2019) 3715. https://doi.org/10.1002/qj.3651.

[21] B. Elliston, I. MacGill, A. Prasad & M. Kay, "Spatio-temporal characterization of extended low direct normal irradiance events over Australia using satellite derived solar radiation data", Renewable Energy **74** (2015) 633. https://doi.org/10.1016/j.renene.2014.08.067.

[22] K. K. K. Cheung, S. Chooprateep & J. Ma, "Spatial and temporal patterns of solar absorption by clouds in Australia as revealed by exploratory factor analysis", Solar Energy **111** (2015) 53. https://doi.org/10.1016/j.solener.2014.10.014.

[23] A. Troccoli & J. J. Morcrette, "Skill of direct solar radiation predicted by the ECMWF global atmospheric model over Australia", Journal of Applied Meteorology and Climatology **53** (2014) 2571. https://doi.org/10.1175/JAMC-D-14-0074.1.

[24] S. Jerez, R. M. Trigo, S. M. Vicente-Serrano, D. Pozo-Vázquez, R. Lorente-Plazas, J. Lorenzo-Lacruz, F. Santos-Alamillos & J. P. Montávez, "The impact of the north atlantic oscillation on renewable energy resources in Southwestern Europe", Journal of Applied Meteorology and Climatology **52** (2013) 2204. https://doi.org/10.1175/JAMC-D-12-0257.1.

[25] G. Colantuono, Y. Wang, E. Hanna & R. Erdélyi, "Signature of the north atlantic oscillation on British solar radiation availability and PV potential: the winter zonal seesaw", Solar Energy **107** (2014) 210. https://doi.org/10.1016/j.solener.2014.05.045.

[26] L. T. Abiem, T. Igbawua & S. I. Aondoakaa, "Spatio-temporal assessment of climate in response to solar radiation changes over Nigeria using satellite data", International Journal of Energy and Environmental Science **5** (2020) 40. https://doi.org/10.11648/j.ijees.20200502.12.

[27] T. Igbawua, A. A. Tyovenda, T. Sombo & I. M. Echi, "Spatio-temporal assessment of aerosol-induced atmospheric heating rates in Nigeria", Journal of the Nigerian Society of Physical Sciences **7** (2025) 1918. https://doi.org/10.46481/jnsps.2025.1918.

[28] H. E. Beck, T. R. McVicar, N. Vergopolan, A. Berg, N. J. Lutsko, A. Dufour, Z. Zeng, X. Jiang, A. I. J. M van Dijk & D. G. Miralles, "High-resolution (1 km) Köppen-Geiger maps for 1901–2099 based on constrained CMIP6 projections", Scientific Data **10** (2023) 724. https://doi.org/10.1038/s41597-023-02549-6.

[29] A. A. Prasad, R. A. Taylor & M. Kay, "Assessment of direct normal irradiance and cloud connections using satellite data over Australia", Applied Energy **143** (2015) 301. http://dx.doi.org/10.1016/j.apenergy.2015.01.050.

[30] M. Journée, R. Müller & C. Bertrand, "Solar resource assessment in the Benelux by merging Meteosat-derived climate data and ground measurements", Solar Energy **86** (2012) 3561. https://doi.org/10.1016/j.solener.2012.06.023.

[31] N. G. Loeb, S. Kato, W. Su, T. Wong, F. G. Rose & D. R. Doelling, "Advances in understanding top-of-atmosphere radiation variability from satellite observations", Surveys in Geophysics **33** (2012) 359. https://doi.org/10.1007/s10712-012-9175-1.

[32] B. F. Murphy & B. Timbal, "A review of recent climate variability and climate change in southeastern Australia", International Journal of Climatology **28** (2008) 859. https://doi.org/10.1002/joc.1627.

[33] A. A. Prasad & R. Davies, "Decadal changes in thin cirrus height measured by MISR", AIP Conference Proceedings **1531** (2013) 400. https://doi.org/10.1063/1.4804791.

[34] S. T. Ogunjo, A. A. Obafaye & A. B. Rabiu, "Solar energy potentials in different climatic zones of Nigeria", IOP Conference Series: Materials Science and Engineering **1032** (2021) 012040. https://doi.org/10.1088/1757-899X/1032/1/012040.

[35] O. S. Ohunakin, M. S. Adaramola, O. M. Oyewola, O. J. Matthew & R. O. Fagbenle, "The effect of climate change on solar radiation in Nigeria", Solar Energy **116** (2015) 272. https://doi.org/10.1016/j.solener.2015.03.027.
[36] M. D. Dogara, M. K. O. Onwumere, S. Turang, P. Joshua & I. A. Joseph, "The trends in temperature and solar irradiance for Zaria, north western, Nigeria, between 1986 and 2015", Science World Journal **12** (2017) 25. https://scienceworldjournal.org/article/view/17901.
[37] T. Sato, F. Kimura & A. S. Hasegawa, "Vegetation and topographic control of cloud activity over arid/semiarid Asia", Journal of Geophysical Research: Atmospheres **112** (2007) 1. https://doi.org/10.1029/2006JD008129.
[38] D. O. Edokpa, P. N. Ede, J. Brown, A. J. Adeyemi & I. U. Pukiche, "The Nigeria climate zones: variability, trends and analysis from era-interim data (2010-2015)", International Journal of Climate Research **8** (2024) 1. https://doi.org/10.18488/112.v8i1.3804.
[39] D. W. Medugu, S. B. Ibrahim & E. Yonanna, "The influence of some meteorological parameters on solar radiation in Yola, Adamawa State, Nigeria", Adamawa State University Journal of Scientific Research **5** (2017) 153. https://www.adsujsr.com/.
[40] R. J. Davy & A. Troccoli, "Continental-scale spatial optimisation of a solar irradiance monitoring network", Solar Energy **109** (2014) 36. https://doi.org/10.1016/j.solener.2014.08.026.
[41] E. J. Bala, J. O. Ojosu & I. H. Umar, "Government policies and programmes on the development of solar-PV sub-sector in Nigeria", Nigerian Journal of Renewable Energy **8** (2000) 1. https://scholar.google.com/scholar?hl=en&as_sdt=0,5&cluster=13510257450420325907.
[42] IEA: International Energy Agency, World Energy Outlook 2010, IEA Paris, France, 2010. https://www.iea.org/reports/world-energy-outlook-2010.
[43] M. J. McPhaden, S. E. Zebiak & M. H. Glantz, "ENSO as an integrating concept in earth science", Science **314** (2006) 1740. https://doi.org/10.1126/science.1132588.